

Svoboda P, Dvorackova M, Svobodova D. Influence of biodegradation on crystallization of poly (butylene adipate-co-terephthalate). *Polymers for Advanced Technologies*. 2019;30(3):552-562. <https://doi.org/10.1002/pat.4491>

Influence of biodegradation on crystallization of poly(butylene adipate-co-terephthalate)

Petr Svoboda^{1*}, Marie Dvorackova², Dagmar Svobodova³

¹ Department of Polymer Engineering, Faculty of Technology, Tomas Bata University in Zlin, Vavreckova 275, 762 72 Zlin, Zlin, Czech Republic

²Department of Environmental Engineering, Faculty of Technology, Tomas Bata University in Zlin, Vavreckova 275, 762 72 Zlin, Czech Republic

³ Faculty of Humanities, Tomas Bata University in Zlin, Stefanikova 5670, 760 01, Zlin, Czech Republic

* Corresponding author:

E-mail address: svoboda@utb.cz (P. Svoboda)

Abstract

The biodegradation of aromatic-aliphatic biodegradable polyester poly(butylene adipate-co-terephthalate) (PBAT) was studied under mesophilic (37°C) and thermophilic (55°C) anaerobic conditions. Anaerobic sludge from municipal wastewater treatment plant was utilized as an inoculum. Non-isothermal crystallization kinetics of PBAT before and after biodegradation was explored by differential scanning calorimetry (DSC). Under mesophilic anaerobic conditions (37°C) the biodegradation after 126 days was only 2.2 %, molecular weight changed from 93000 to 25500 g/mol and the crystallization behavior was changed only slightly. However, biodegradation under thermophilic anaerobic conditions (55°C) caused much bigger changes: biodegradation according to biogas production reached after 126 days 8.3 %, molecular weight changed from 93000 to 9430 g/mol and the crystallization behavior was changed significantly. While T_m increased only slightly, T_c on the other hand increased significantly for the sample after biodegradation at 55°C. Also the crystallization rate was slower (particularly at lower cooling rates), but crystallinity was slightly higher. The diffraction pattern was observed by X-ray diffraction (XRD).

Keywords: poly(butylene adipate-co-terephthalate); anaerobic thermophilic sludge; crystallization; GPC; DSC

Introduction

Biodegradable polymers are at present more attractive than ever since they are environmentally friendly. An aromatic-aliphatic biodegradable co-polyester, poly(butylene adipate-co-butylene terephthalate) (PBAT) has been produced by BASF under the trade name Ecoflex[®]. PBAT is not only biodegradable, but it has also excellent thermal and mechanical properties, thus it is used in applications such as agricultural materials (mulch film), compost bags, lamination materials, food packaging, bags for organic waste or carrier bags [1].

In the past decades, anaerobic metabolization has become significant in the biological treatment of organic household wastes, frequently applied in existing composting plants. Several authors have investigated biodegradation of Ecoflex[®] in different composting [2-13] and other environments such as soil burial [2-4, 11, 14-17]. Only limited research has been reported on the biodegradation behaviour of the PBAT in anaerobic environment, and the respective degradation behaviour under anaerobic thermophilic conditions [11, 18-21]. Perz et al. [22] have revealed that typical anaerobic sludge can hydrolyze PBAT to some level, despite the fact that the PBAT hydrolysis rate is not very high.

Both biotic and abiotic factors of the environment, such as moisture, temperature, bio-surfactants, pH, and enzymes influence the biodegradability of biodegradable polymers; and so do the internal polymer characteristics, such as crystallinity, chain flexibility, heterogeneity, regularity, molecular weight and functional groups [15, 23]. In the microbial mineralization of polyesters, the first step to produce oligomers and monomers is hydrolysis by extracellular enzymes. Smaller molecules can be further digested in microbial cells. The sensitivity to an enzymatic decomposition greatly rises when the crystalline domains have their melting point less than 30 - 40 °C above the biodegradation temperature [20, 24].

The biodegradability of polymers is affected firstly by their chemical structure, especially by the functional groups and by hydrophobicity-hydrophilicity balance, secondly by the ordered structure such as orientation, crystallinity, and other morphological properties [3, 10, 14, 25-27]. Crystalline regions in a semicrystalline polymer are less susceptible to degradation than amorphous regions, because the rate of water penetration is lower in the crystalline regions than in the amorphous regions as the polymer chains are much more closely arranged in crystal lamellae compared to the loose arrangement in amorphous regions.

Polymer crystallization kinetics must be explored from both points of view: theoretical and practical. The mechanism of generation of the polymer crystal lamellae is significant in the theoretical part. The practical part of polymer crystallization dwells in the effect to which crystallinity influences the chemical and physical properties of polymers [28].

Ergoz et al. [29] discovered the great influence of molecular weight on crystallinity and crystallization rate. Crystallization rate was found to have a maximum at molecular weight around 10^5 g/mol. Crystallinity below molecular weight 10^5 g/mol was almost constant and above 10^5 g/mol it decreased steadily. Molecular weight always decreases during biodegradation. Therefore, one can expect changes in crystallization behavior after biodegradation. This assumption led to a detailed study of non-isothermal crystallization kinetics of PBAT after biodegradation at low and high temperatures.

Biodegradability, thermal and mechanical properties are closely related to polymer crystal structure [30]. In relation to a higher level of hydrolysis manifested by PBAT at elevated temperatures [14] and consequently a possible rise in the degree of biodegradation in an anaerobic environment, we investigated the behavior of PBAT in thermophilic anaerobic sludge at 55°C. Similar biodegradation was carried out also at 37°C in order to compare both outcomes. Secondly, melting temperature T_m and crystallization temperature T_c changes were examined, and thirdly, differential scanning calorimetry (DSC) was applied to evaluate the kinetics of non-isothermal crystallization. Even though PBAT has been excessively studied under aerobic conditions, kinetics of crystallization after biodegradation in thermophilic anaerobic sludge was not yet analyzed.

Materials and methods

Materials

PBAT, trade name Ecoflex®, was supplied by BASF, Germany; in the form of a 70 μm thick film. The material has a number-average molecular weight (M_n) of 93000 g/mol, as determined by gel permeation chromatography (GPC). Its melting point is 122.2 °C according to differential scanning calorimetry (DSC) during the first heating scan at 10°C/min. Organic carbon content (w_c) equalled 62.4%, as determined by elemental analysis.

The contents of aliphatic and aromatic constituents in Ecoflex were identified by ^1H -NMR measurement [26] of Ecoflex solution with the solvent being deuterated chloroform at concentration of 50 mg/mL. This method revealed 24.2 mol% of aromatic and 75.8 mol% of aliphatic components in Ecoflex. [17]

We have purchased **microcrystalline cellulose** from Sigma-Aldrich. It was in powder form with particles smaller than 20 μm , and it was used in the biodegradation tests as control.

We prepared **nutrient medium** in accordance with CSN ISO 11743 as follows: Na₂HPO₄ (1.120 g/L), KH₂PO₄ (0.270 g/L), MgCl₂·6H₂O (0.100 g/L), NH₄Cl (0.530 g/L), FeCl₂·4H₂O (0.020 g/L), CaCl₂·2H₂O (0.075 g/L).

Applied inocula

- a) *mesophilic anaerobic (MA) sludge (37°C)* from the municipal wastewater treatment plant Zlin – Malenovice
- b) *thermophilic anaerobic (TA) sludge*, prepared from the MA sludge by increasing its temperature from 37 °C to 55°C for 15 days. The amount of 1.5 L of MA sludge was centrifuged at 3,600 rpm for 10min then it was suspended in nutrient medium into a 2-L glass bottle sealed with caps equipped with a gas-tight sampling valve. Consequently, pH, oxidation-reduction potential (ORP), total solids, and volatile solids in sludge were recorded. CH₄ content in biogas (methane and carbon dioxide) was analyzed using gas chromatography. The MA sludge was then kept in thermostat at 55 °C for 15 days and it changed to thermophilic anaerobic sludge which produced biogas with CH₄ content than 60% (Table 1).

Biodegradation of PBAT in MA sludge at 37 °C

Film samples (5 x 5 mm) with weight about 100 mg were put into 250-mL glass gas-tight bottles sealed with caps equipped with a gas-tight sampling valves. The amounts of 100 mL MA sludge containing 2.7 g·L⁻¹ of total solids were added and bottles were stored at (37 ± 2) °C. Biogas production was recorded once a week by gas chromatograph. Sampling amounts of 100 µl were taken and injected into a gas chromatograph (GC) (Agilent 7890), equipped with Porapak Q (1.829 m length, 80/100 MESH), carrier gas helium, flow 53 mL min⁻¹, column temperature 50 °C, thermal conductivity detector. CH₄ and CO₂ contents were calculated from the calibration curve obtained using a calibration gas mixture with declared composition (Linde). In the final stage of our experiment, we determined pH, oxidation-reduction potential (ORP), sample weight loss and inorganic carbon concentration in the liquid phase using Shimadzu 5000A device.

The degree of total biodegradation D_t (%) of PBAT samples was calculated according to Equation 1:

$$D_t = \frac{m_g + m_l}{m_v} \times 100 \quad (1)$$

where

m_g (mg) is carbon released in biogas in the form of CH₄ and CO₂

m_l (mg) is carbon found in liquid form as carbonate,

and m_v (mg) is theoretical carbon input in the tested samples.

Biodegradation of PBAT in TA sludge at 55 °C

Film samples (5 x 5 mm) with weight about 50 mg were put into 100-mL glass gas-tight bottles and 50 mL of TA sludge was added. Bottles were stored at (55 ± 2) °C. Biodegradation was recorded once a week as the produced biogas (methane and carbon dioxide) was analyzed in GC. The degree of biodegradation D_t (%) of tested samples was then calculated using Eq. (1).

Determination of weight loss in Ecoflex

The sample weight loss was monitored during the biodegradation. Initially the polyester was incubated, cleansed by distilled water and finally dried in the desiccator to the constant mass. The weight loss (ΔW) of the samples was evaluated from the weight of each sample before and after biodegradation. Three samples were always averaged.

Thermal Analysis

Differential scanning calorimetry (Mettler Toledo DSC, closed aluminum crucibles) identified characteristic peaks. About 7 mg of the sample was inserted into the crucible and heat flow was measured in a N₂ (flow rate 20 mL/min) in the temperature range -90 to +200 °C at rates 10, 20, 30, 40 and 50 °C/min. An example of one experiment with heating and cooling rates 40 °C/min is as follows: heating from 25 °C to 200 °C at rate 40 °C/min (first heating), then cooling from 200 °C to -90 °C at rate 40 °C/min, and lastly heating from -90 °C to 200 °C at rate 40 °C/min (second heating). Three measurements were always averaged and the standard deviation was less than 2%.

Gel permeation chromatography

Gel permeation chromatography (GPC) was used to get the weight average molecular weight (M_w) and molecular weight distribution before and after biodegradation. HT-GPC 220 system

(Agilent) with dual detection system (“VIS” viscosity detectors and “RI” refractive index) was used. THF was used as a solvent, concentration was about 2 mg/mL. Detection and separation were performed in mixed columns from Polymer Laboratories, 300 × 7.8 mm. Solvent was THF, temperature 40°C, loading volume 100 µL, flow rate 1.0 mL/min. Calibration was performed with narrow polystyrene standards (Polymer Laboratories Ltd., UK) having molecular weight in range 580 to 3,000,000 g/mol.

XRD analysis

PBAT films were analyzed by X-ray diffractometer X’Pert PRO from *PANalytical*. 2 θ range was 5–60°, steps were 0.05°, time 5s, radiation Cu K α ($\lambda=0.154$ nm), 40 kV and 30 mA.

Results and Discussion

Biodegradation of PBAT in anaerobic mesophilic sludge (37 °C)

Figure 2 illustrates the level of biodegradation of PBAT by the help of biogas production (Dg) that was evaluated from biogas released from the sludge during anaerobic biodegradation at 37°C and 55°C. The value of Dg cannot indicate the value of total biodegradation (D_t) because part of the carbon is in the liquid phase (as bicarbonates) and therefore is was evaluated in the end of the experiment. Total biodegradation (D_t) was calculated with the help of Equation (1).

Results show that PBAT almost does not at decomposed at 37°C (in mesophilic anaerobic sludge). The value of D_t for PBAT samples (total anaerobic biodegradability) was 2.2 % (see Table 2). Similar results were published by many authors [18, 21].

Biodegradation of PBAT in anaerobic thermophilic sludge (55 °C)

Table 2 summarizes the test results. Evaluated parameters of the biodegradation of the PBAT samples were expressed as total decomposition (D_t) and biogas production (Dg). These parameters were evaluated from the carbon production in biogas and inorganic carbon (liquid phase) and biodegradation through the loss in mass of the sample (ΔW).

Results shown in Fig. 2 and listed in Table 2 are in agreement with results from Abou-Zeid et al. [18] who described difficult decomposition of PBAT in anaerobic thermophilic sludge. In our case after 126 days Ecoflex decomposed by only 8.3 %. In an aerobic environment during composting at temperature 58°C, PBAT reaches a higher, cca 15.8 %, degree of biodegradation, e.g. during 120 days according to Wu et al.[9]. The increase of temperature thus does not

influence final biodegradation of PBAT in anaerobic sludge, but it strongly influences firstly the hydrolysis degree, secondly the change in molar mass and thirdly the thermal properties as illustrated below.

Better degradability at elevated temperatures results firstly from abiotic hydrolysis and from different microorganisms at thermophilic conditions, and secondly from higher sensitivity of the polymer chains to the degradation enzymes because of enhanced chain mobility.

Thermal behaviour of PBAT after biodegradation in mesophilic (37 °C) and thermophilic anaerobic condition (55 °C)

Nonisothermal crystallization by differential scanning calorimetry

PBAT samples were initially melted and then cooled at various rates (range 10 – 50 °C/min). Exothermic curves of the heat flow were recorded. Data analysis was done according to sequence disclosed by Liu et al [31]. Mechanism of the phase transition is strongly influenced by the cooling rate. The relative crystallinity (X_t) was calculated according to Equation 2:

$$X_t = \int_{T_0}^T \left(\frac{dH_c}{dT} \right) dT / \int_{T_0}^{T_\infty} \left(\frac{dH_c}{dT} \right) dT \quad (2)$$

where T_0 is onset of crystallization and T_∞ is the the end of crystallization, and dH_c/dT is the heat flow at temperature T. Crystallization time t is given by:

$$t = \frac{T_0 - T}{\varphi} \quad (3)$$

where φ is the cooling rate.

Fig. 3 illustrates non-isothermal crystallization measured by DSC. Firstly, there is the quite remarkable influence of cooling rate on the peak position. With increasing cooling rate, the crystallization temperature T_c shifts towards lower temperatures. This T_c shift (due to cooling rate) is quite small for PBAT degraded at 55°C. PBAT samples before and after biodegradation at 37°C exhibit quite similar crystallization behavior; however, the peaks for sample degraded at 55°C shifted significantly towards higher temperatures (compared to the original sample).

Weng et al. [3] studied biodegradation of PBAT in soil and they observed a shift of T_c towards lower temperature (from 80 to 73°C). On the other hand, Muthuraj et al. [14] who performed a hydrolysis of PBAT at 50°C for 30 days, observed an increase in T_c (from 81.11 to 96.50°C). Our results are in agreement with Muthuraj et al. In our case, after biodegradation, the T_c shifted also towards higher temperatures.

The temperature versus heat flow curves (see Figure 3 a,b,c) were recalculated to time vs. heat flow curves (see Figure 3 d,e,f) with the help of Eq. 3. Peak area (integral) from time vs. heat flow curves was normalized to sample weight and divided by ΔH_{m100} (114 J/g) [14] to get the crystallinity which is listed in Table 3.

Fig. 4 depicts crystallization and melting behavior just for one rate (40°C/min). The shift of the crystallization peak for the sample degraded at 55°C is very large (45.18°C), while the shift of the sample degraded at 37°C is only very small (2.50°C). One reason for a T_c shift could be a shift in melting temperature T_m . This was investigated in Fig. 4b. The melting temperature shifted towards higher temperature; however, the shift was very moderate (2.84 and 4.30°C). A small increase in melting temperature can be attributed to a small increase in the lamellar size that was caused most likely by the healing of the imperfections during the long-term annealing at elevated temperature. In contrast the huge shift in crystallization temperature (45.18°C) must have another cause than the T_m shift (4.30°C). The culprit is most likely an increased nucleation rate. The reason for the increased nucleation rate could be either lower molecular weight or presence of inhomogeneities due to biodegradation in sludge, or it could be the influence of both factors. The inhomogeneities could have origin in remaining parts of the microorganisms.

Fig. 5 shows the influence of heating and cooling rates on melting (T_m) and crystallization (T_c) temperatures. Firstly, there is a small increase in melting temperatures (at the top of the graph) due to biodegradation. The crystallization temperature increased moderately for samples degraded at 37°C; however, there is a huge shift of crystallization temperature towards higher temperatures for samples degraded at 55°C. One can notice quite a small rate dependence of T_m compared to large rate dependence for T_c . Numerical values of T_m and T_c are listed in Table 3 where crystallinity X is also shown. Crystallinity increased only slightly for samples after biodegradation at 55°C. Increased crystallinity suggests that the amorphous regions are being degraded first [10]. It is worth to notice that Figs. 3 and 4 are shown just for the measurement of one selected sample while Fig. 5 summarizes the average values and standard deviations for 3 DSC measurements.

The crystallization kinetics was analyzed in detail and initially the relative crystallinity (X_t) was plotted as a function of time in Fig. 6. When we compare the original sample with the sample degraded at 37°C, the crystallization kinetics is quite similar. Even the sample degraded at 55°C exhibits similar crystallization kinetics for fast cooling rates (50, 40 and 30°C/min). However, at slower cooling rates (20 and 10°C/min) the crystallization kinetics is remarkably slower for the sample degraded at 55°C. While e.g. at 10°C/min rate it takes about 150s to complete the crystallization of the original sample, it takes more than 400s to complete the crystallization of the sample degraded at 55°C.

The comparison of crystallization kinetics is clearly visible in Fig. 7 for the cooling rate 10°C/min. While the crystallization kinetics for the original sample and the one degraded at 37°C are almost identical, the sample degraded at 55°C is significantly slower. After the biodegradation at 55°C, the diffusion process (or mobility) of the polymer chains towards the growing front of a lamella could be slower. Another explanation could be in inhomogenities introduced from the sludge during biodegradation that act as obstacles during the growth of lamellae. The lamellae have to go around the obstacle which slows down the overall crystallization process. One important factor is also the fact that the crystallization proceeded at higher temperature (closer to T_m) which generally decreases the crystallization rate.

The development of relative crystallinity in time is expressed by Avrami equation and we used it to analyze crystallization kinetics [32]:

$$1 - X_t = \exp(-Zt^n) \quad (4)$$

where X_t is relative crystallinity increasing in time t . Z is a constant relating to crystallization rate and n is the Avrami constant relating to nucleation and growth. Equation (4) can be written in double logarithmic form:

$$\ln[-\ln(1 - X_t)] = \ln Z - n \ln t \quad (5)$$

Avrami equation was originally developed for the study of isothermal crystallization of low molecular substances [33]. The n index is an integer ranging from 1 to 4, and is related to nucleation and growth parameters as follows [34]:

$$n = \alpha + (d/p) \quad (6)$$

where n is the Avrami index, α is the nucleation index ($\alpha=1$ for homogeneous nucleation and 0 for heterogeneous nucleation), d is the dimensionality of crystal growth (with values 1, 2 and

3 for one-, two- and three- dimensional growths, respectively), and p is the growth index ($p = 1$ for interface-controlled growth, and 0.5 for diffusion-controlled growth). Later, Avrami equation was also applied by many authors to evaluate the kinetics of polymer crystallization under nonisothermal conditions [33]. In this case, however, the Avrami parameters do not have the same physical meaning as in the case of isothermal crystallization kinetics, because temperature change affects the rate of both nuclei formation and spherulite growth [35]. They are rather used as adjustable parameters in fitting the Avrami equation to experimental data. Nevertheless these parameters are quite useful in tracking changes in polymer crystallization due to sample modification such as biodegradation [36, 37] and there is a very good correlation between half time of crystallization $t_{1/2}$ with Avrami normalized rate constant K as it is shown below.

One can obtain one-half of crystallization $t_{1/2}$ from graphs shown in Figs. 6 and 7 when the crystallinity curve reaches 50% value (or $X_t=0.5$). This $t_{1/2}$ value is plotted as a function of the cooling rate in Fig. 9. Firstly, the $t_{1/2}$ values are quite similar for the original sample and the one degraded at 37°C. However, one can notice quite a large difference in $t_{1/2}$ values for samples degraded at 55°C crystallized at slower cooling rates (10 and 20°C/min), the crystallization took considerably longer time. Crystallization kinetics can be expressed also as $1/t_{1/2}$ as it is shown in Fig. 9b. Interestingly, the sample which degraded at 55°C shows lower crystallization kinetics for all cooling rates.

From Figure 8 which illustrates $\ln[-\ln(1-X_t)]$ as a function of $\ln t$, one can use the linear portions of the curves (we have used range of relative crystallinity 5-95%) and can get parameters n and Z . These are listed in Table 4. Rate constant Z is commonly used to evaluate the rate of crystallization kinetics, however, n parameter may differ for various samples which can complicate the evaluation of the crystallization kinetics rates of different samples. Consequently, a normalized rate constant K which is independent on Avrami exponent was utilized in Eq. (7)[38]:

$$K = Z^{1/n} \quad (7)$$

Calculated values of normalized rate constant K are given in Table 4. With growing cooling rate, K constant increased for all samples. The original sample and the sample after biodegradation at 37°C show quite similar corresponding K values. In contrast, we can notice substantially different K values for the sample after biodegradation at 55°C at cooling rates 10

°C/min (0.0058 vs. 0.0117 s⁻¹) which indicates about 1/2 crystallization kinetics; this agrees well with $t_{1/2}$ increased from 75.51 to 142.79s obtained by a different kind of data analysis.

It is clear from Table 4 and Figure 9a that sample after biodegradation needs significantly extended time to reach 50% crystallinity, i.e. the crystallization takes much longer time.

The crystallization kinetics rate was described in [39] with the help of $1/t_{1/2}$ value. Figure 9b illustrates $1/t_{1/2}$ values as a function of cooling rate (before and after biodegradation) and it confirms slower crystallization as expressed by the normalized rate constant.

These results can be compared with [28, 40] where the influence of molecular weight on crystallization of poly(tri-methylene-terephthalate), another polyester, was observed. The conclusion was that polyester with lower M_w has significantly lower T_c and that the crystallization takes significantly longer time. Additionally, the nucleation density grows with an increasing M_w . In our experiment, biodegradation resulted in decreased molecular weight and we have detected slower crystallization. However, after biodegradation the T_c substantially increased. Muthuraj et al. [14] explained the shift in T_c towards higher temperature by increased nucleation caused by the presence of oligomers.

Gel permeation chromatography

In order to analyze the changes in material at a molecular level (especially chain scission), which could not be detected by analyzing of product of mineralization, GPC measurements of PBAT after biodegradation was carried out and compared with non-degraded sample (Fig. 10). Obtained data showed the significant shift in molecular weight towards lower values after biodegradation experiment even though final mineralization reaches 8,3 % for sample after biodegradation at 55°C. The average weight molecular weight M_w declined from 93000 g/mol in original sample to 25500 (37°C) and to 9430 g/mol (55°C) and polydispersity index (PDI) changed from 2.48 (original sample) to 2.56 (37°C) and to 1.89 for the sample after biodegradation at 55°C. This considerable drop of molecular weight suggested hydrolysis of ester bonds by microorganisms during biodegradation (Fig.1). However, despite dramatic reduction in the length of the polymer chains of PBAT, it is likely that the particles are still too bulky to penetrate the cell membrane of microorganisms, thus they have to be shortened even more to permit assimilation and final microbial mineralization.

Systematic change in molecular weight (93000, 25500, 9430 g/mol) corresponds well with systematic change in melting point T_m shown in Figure 5. The interesting was the abrupt

change in crystallization temperature and crystallization kinetics (see Figure 6) from sample 37°C to 55°C. Apparently in this range of low molecular weight (25500, 9430 g/mol) the crystallization is influenced much more than in range (93000 – 25500 g/mol). This agrees well with the findings of Ergoz et al. [29] who found only small change in crystallization kinetics for polyethylene samples with molecular weight in range 30000-100000 g/mol but a huge difference in crystallization kinetics in range 8000-30000 g/mol. In their case with decreasing molecular weight in range 8000-30000 g/mol the rate of crystallization decreased tremendously (10-100x).

XRD Analysis

The XRD results of PBAT before and after biodegradation are presented in Fig. 11. PBAT exhibits five different diffraction peaks, with a combination of amorphous and crystalline structures. The crystal peaks for the sample before biodegradation were observed at 16.3°, 17.5°, 20.5°, 23.1 and 24.9° corresponding to the planes of (011), (010), (101), (100) and (111), respectively [41].

In angle ranges 5-14° and 24-35° the intensity increases systematically for original sample, 37°C and 55°C samples. However, in angle range 14-24° the original sample has peaks between the 37°C and 55°C samples. The biodegradation causes slight increase in overall crystallinity due to partial assimilation of amorphous phase by microorganisms, but the structure of remaining crystals is not influenced significantly.

Conclusion

Biodegradation of aromatic-aliphatic copolymer poly(butylene adipate-co-terephthalate) (PBAT, Ecoflex[®]) was studied in mesophilic (37°C) and thermophilic anaerobic sludge (55°C). It was confirmed that pure Ecoflex[®] almost does not decompose in anaerobic thermophilic sludge (only 2.2 %) based on biogas production. However, in case of thermophilic anaerobic degradation the biogas production was higher (e.g. 8.3 % after 126 days); which means increased biological degradation of PBAT.

The average molecular weight M_w declined from 93000 g/mol in the original sample to 25500 g/mol after biodegradation at 37°C and to 9430 g/mol after biodegradation at 55°C. This considerable drop in molecular weight suggested the hydrolysis of ester bonds at elevated temperature during biodegradation.

The crystallization kinetics of PBAT was studied in detail by DSC after biodegradation in mesophilic and thermophilic anaerobic degradation. It was also analyzed using Avrami equation. When we compare the original sample with the sample degraded at 37°C the crystallization kinetics was quite similar. However, the sample degraded at 55°C exhibited quite different crystallization behavior.

Both concurrent impacts, higher temperature and biodegradation, cause decrease in the polymer chains' length that normally leads to a decreased crystal size; however, in our case the melting point increased. One possibility how this phenomenon could be interpreted is an increase in the crystal size according to Gibbs-Thompson equation [42]. Another possibility is a change in copolymer composition after biodegradation due to decreasing content of aliphatic part of polymer chain which could be preferably hydrolyzed during biodegradation at 55°C [22]. Also the crystallinity slightly increased after biodegradation.

Biodegradation at 55°C led to a significant change in crystallization behavior. Crystallization kinetics was slower and T_c shifted towards higher temperatures that could be interpreted by higher nucleation and/or by a change in copolymer composition (higher content of butylene terephthalate in PBAT).

References

- [1] Bilck AP, Grossmann MVE, Yamashita F. Biodegradable mulch films for strawberry production. *Polym Test*. 2010;(29)(4):471-476.
- [2] Mondal D, Bhowmick B, Mollick MMR, Maity D, Saha NR, Rangarajan V, et al. Antimicrobial Activity and Biodegradation Behavior of Poly(butylene adipate-co-terephthalate)/Clay Nanocomposites. *J Appl Polym Sci*. 2014;131(7).
- [3] Weng YX, Jin YJ, Meng QY, Wang L, Zhang M, Wang YZ. Biodegradation behavior of poly(butylene adipate-co-terephthalate) (PBAT), poly(lactic acid) (PLA), and their blend under soil conditions. *Polym Test*. 2013;32(5):918-926.
- [4] Saadi Z, Cesar G, Bewa H, Benguigui L. Fungal Degradation of Poly(Butylene Adipate-Co-Terephthalate) in Soil and in Compost. *J Polym Environ*. 2013;21(4):893-901.
- [5] Muniyasamy S, Reddy MM, Misra M, Mohanty A. Biodegradable green composites from bioethanol co-product and poly(butylene adipate-co-terephthalate). *Ind Crop Prod*. 2013;43:812-819.
- [6] Lee JJ, Jeon JY, Park JH, Jang Y, Hwang EY, Lee BY. Preparation of high-molecular-weight poly(1,4-butylene carbonate-co-terephthalate) and its thermal properties. *Rsc Adv*. 2013;3(48):25823-25829.
- [7] Wu CS. Utilization of peanut husks as a filler in aliphatic-aromatic polyesters: Preparation, characterization, and biodegradability. *Polym Degrad Stabil*. 2012;97(11):2388-2395.
- [8] Intaraksa P, Rudeekit Y, Siriyota P, Chaiwutthinan P, Tajan M, Leejarkpai T. The Ultimate Biodegradation of The Starch Based Biodegradable Plastics. *Adv Mater Res-Switz*. 2012;506:327-330.
- [9] Wu CS. Process, Characterization and Biodegradability of Aliphatic Aromatic Polyester/Sisal Fiber Composites. *J Polym Environ*. 2011;19(3):706-713.
- [10] Kijchavengkul T, Auras R, Rubino M, Selke S, Ngouajio M, Fernandez RT. Biodegradation and hydrolysis rate of aliphatic aromatic polyester. *Polym Degrad Stabil*. 2010;95(12):2641-2647.
- [11] Hermann BG, Debeer L, De Wilde B, Blok K, Patel MK. To compost or not to compost: Carbon and energy footprints of biodegradable materials' waste treatment. *Polym Degrad Stabil*. 2011;96(6):1159-1171.
- [12] Kijchavengkul T, Auras R, Rubino M, Ngouajio M, Fernandez RT. Assessment of aliphatic-aromatic copolyester biodegradable mulch films. Part II: Laboratory simulated conditions. *Chemosphere*. 2008;71(9):1607-1616.
- [13] Witt U, Einig T, Yamamoto M, Kleeberg I, Deckwer WD, Muller RJ. Biodegradation of aliphatic-aromatic copolyesters: evaluation of the final biodegradability and ecotoxicological impact of degradation intermediates. *Chemosphere*. 2001;44(2):289-299.
- [14] Muthuraj R, Misra M, Mohanty AK. Hydrolytic degradation of biodegradable polyesters under simulated environmental conditions. *J Appl Polym Sci*. 2015;132(27).
- [15] Kijchavengkul T, Auras R, Rubino M, Alvarado E, Montero JRC, Rosales JM. Atmospheric and soil degradation of aliphatic-aromatic polyester films. *Polym Degrad Stabil*. 2010;95(2):99-107.
- [16] Someya Y, Kondo N, Shibata M. Biodegradation of poly(butylene adipate-co-butylene terephthalate)/Layered-Silicate nanocomposites. *J Appl Polym Sci*. 2007;106(2):730-736.
- [17] Stloukal P, Verney V, Commereuc S, Rychly J, Matisova-Rychla L, Pis V, et al. Assessment of the interrelation between photooxidation and biodegradation of selected polyesters after artificial weathering. *Chemosphere*. 2012;88(10):1214-1219.

- [18] Abou-Zeid DM, Muller RJ, Deckwer WD. Biodegradation of aliphatic homopolyesters and aliphatic - Aromatic copolyesters by anaerobic microorganisms. *Biomacromolecules*. 2004;5(5):1687-1697.
- [19] Biundo A, Hromic A, Pavkov-Keller T, Gruber K, Quartinello F, Haernvall K, et al. Characterization of a poly(butylene adipate-co-terephthalate)-hydrolyzing lipase from *Pelosinus fermentans*. *Appl Microbiol Biot*. 2016;100(4):1753-1764.
- [20] Perz V, Hromic A, Baumschlager A, Steinkellner G, Paykov-Keller T, Gruber K, et al. An Esterase from Anaerobic *Clostridium hathewayi* Can Hydrolyze Aliphatic-Aromatic Polyesters. *Environ Sci Technol*. 2016;50(6):2899-2907.
- [21] Shi B, Shlepr M, Palfery D. Effect of Blend Composition and Structure on Biodegradation of Starch/Ecoflex-Filled Polyethylene Films. *J Appl Polym Sci*. 2011;120(3):1808-1816.
- [22] Perz V, Baumschlager A, Bleymaier K, Zitzenbacher S, Hromic A, Steinkellner G, et al. Hydrolysis of synthetic polyesters by *Clostridium botulinum* esterases. *Biotechnol Bioeng*. 2016;113(5):1024-1034.
- [23] Tan FT, Cooper DG, Maric M, Nicell JA. Biodegradation of a synthetic co-polyester by aerobic mesophilic microorganisms. *Polym Degrad Stabil*. 2008;93(8):1479-1485.
- [24] Marten E, Muller RJ, Deckwer WD. Studies on the enzymatic hydrolysis of polyesters. II. Aliphatic-aromatic copolyesters. *Polym Degrad Stabil*. 2005;88(3):371-381.
- [25] Dong WF, Zou BS, Yan YY, Ma PM, Chen MQ. Effect of Chain-Extenders on the Properties and Hydrolytic Degradation Behavior of the Poly(lactide)/Poly(butylene adipate-co-terephthalate) Blends. *Int J Mol Sci*. 2013;14(10):20189-20203.
- [26] Herrera R, Franco L, Rodriguez-Galan A, Puiggali J. Characterization and degradation behavior of poly(butylene adipate-co-terephthalate)s. *J Polym Sci Pol Chem*. 2002;40(23):4141-4157.
- [27] Mohanty S, Nayak SK. Aromatic-Aliphatic Poly(butylene adipate-co-terephthalate) Bionanocomposite: Influence of Organic Modification on Structure and Properties. *Polym Composite*. 2010;31(7):1194-1204.
- [28] Wang XS, Yan DY, Tian GH, Li XG. Effect of molecular weight on crystallization and melting of poly(trimethylene terephthalate). 1: Isothermal and dynamic crystallization. *Polym Eng Sci*. 2001;41(10):1655-1664.
- [29] Ergoz E, Fatou JG, Mandelkern L. Molecular-Weight Dependence of Crystallization Kinetics of Linear Polyethylene .1. Experimental Results. *Macromolecules*. 1972;5(2):147-+.
- [30] Shi XQ, Ito H, Kikutani T. Characterization on mixed-crystal structure and properties of poly (butylene adipate-co-terephthalate) biodegradable fibers. *Polymer*. 2005;46(25):11442-11450.
- [31] Liu YF, Wang L, He Y, Fan ZY, Li SM. Non-isothermal crystallization kinetics of poly(L-lactide). *Polym Int*. 2010;59(12):1616-1621.
- [32] Shen HW, Xie BH, Yang W, Yang MB. Non-isothermal crystallization of polyethylene blends with bimodal molecular weight distribution. *Polym Test*. 2013;32(8):1385-1391.
- [33] Kratochvil J, Kelnar I. A simple method of evaluating non-isothermal crystallization kinetics in multicomponent polymer systems. *Polym Test*. 2015;47:79-86.
- [34] Uthaiapan N, Jarntong M, Peng Z, Junhasavasdikul B, Nakason C, Thitithammawong A. Effects of cooling rates on crystallization behavior and melting characteristics of isotactic polypropylene as neat and in the TPVs EPDM/PP and EOC/PP. *Polym Test*. 2015;44:101-111.
- [35] Xu WB, Ge ML, He PS. Nonisothermal crystallization kinetics of polypropylene/montmorillonite nanocomposites. *J Polym Sci Pol Phys*. 2002;40(5):408-414.
- [36] Qiu ZB, Ikehara T, Nishi T. Crystallization behaviour of biodegradable poly(ethylene succinate) from the amorphous state. *Polymer*. 2003;44(18):5429-5437.

- [37] Xu WB, Liang GD, Zhai HB, Tang SP, Hang GP, Pan WP. Preparation and crystallization behaviour of PP/PP-g-MAH/Org-MMT nanocomposite. *Eur Polym J.* 2003;39(7):1467-1474.
- [38] Martinez-Palau M, Franco L, Puiggali J. Nonisothermal crystallization studies on poly(4-hydroxybutyric acid-alt-glycolic acid). *J Polym Sci Pol Phys.* 2008;46(2):121-133.
- [39] Liu FY, Xu CL, Zeng JB, Li SL, Wang YZ. Non-isothermal crystallization kinetics of biodegradable poly(butylene succinate-co-diethylene glycol succinate) copolymers. *Thermochim Acta.* 2013;568:38-45.
- [40] Chen XD, Hou G, Chen YJ, Yang K, Dong YP, Zhou H. Effect of molecular weight on crystallization, melting behavior and morphology of poly(trimethylene terephthalate). *Polym Test.* 2007;26(2):144-153.
- [41] Fukushima K, Rasyida A, Yang MC. Biocompatibility of organically modified nanocomposites based on PBAT. *J Polym Res.* 2013;20(11).
- [42] Pandey A, Toda A, Rastogi S. Influence of Amorphous Component on Melting of Semicrystalline Polymers. *Macromolecules.* 2011;44(20):8042-8055.

Figure captions:

Fig. 1. Hydrolytic degradation of PBAT.

Fig. 2. Degree of biodegradation by biogas production (D_g) of PBAT under mesophilic anaerobic (37°C) and thermophilic anaerobic condition (55°C). D_g (degree of biodegradation by biogas production) is expressed as the percentage of carbon in form of methane and carbon dioxide, generated out of theoretical amount of organic carbon in the polymer. Error bars correspond to twice standard deviation ($n = 3$).

Fig. 3 Nonisothermal crystallization of PBAT at various cooling rates by DSC. (a,d) original sample, (b,e) after biodegradation in mesophilic anaerobic sludge at 37°C (c,f) after biodegradation in thermophilic anaerobic sludge at 55°C.

Fig. 4. Shift of (a) crystallization temperature T_c and (b) melting point T_m for PBAT during second heating and cooling at 40 °C/min.

Fig. 5. Change of crystallization temperature T_c and melting temperature T_m caused by biodegradation of PBAT as a function of heating (cooling) rate.

Fig. 6. Relative crystallinity (X_t) as a function of time during nonisothermal crystallization for PBAT (a) before biodegradation (b) after biodegradation in mesophilic anaerobic sludge at 37°C, (c) after biodegradation in thermophilic anaerobic sludge at 55°C.

Fig. 7. Comparison of relative crystallinity (X_t) development for PBAT before and after biodegradation at cooling rate 10 °C/min.

Fig. 8. Plots according to Avrami's equation for PBAT (a) before biodegradation, (b) after biodegradation at 37 °C, (c) after biodegradation at 55 °C.

Fig. 9 (a) Half time of crystallization $t_{1/2}$ and (b) crystallization kinetics $1/t_{1/2}$ as a function of cooling rate before and after biodegradation under mesophilic (37°C) and thermophilic anaerobic conditions (55°C).

Fig. 10 Molecular weight distribution of PBAT before and after biodegradation under mesophilic (37°C) and thermophilic anaerobic conditions (55°C).

Fig. 11. XRD diffraction patterns for PBAT before and after biodegradation under mesophilic (37°C) and thermophilic anaerobic conditions (55°C).

Table 1

Characterization of the anaerobic sludge before and after 15 days of pre-incubation at 55°C

	Sludge from wastewater treatment plant 37°C	Sludge after 15 days of pre-incubation at 55°C
Total solid (g.L ⁻¹)	23.4	18.9
Volatile solids (%)	48.8	39.8
pH	7.35	7.65
ORP (mV)	-343.2	-333.3
Methane ratio (%)	65.2	71.2

Table 2

Biodegradation after 126 days of PBAT under mesophilic (37°C) and thermophilic anaerobic condition (55°C) according to the degree of biogas production D_g (%), total biodegradation D_t (%) and percentage weight loss (ΔW)

Inoculum	$D_g \pm SD$ [%]	$D_t \pm SD$ [%]	ΔW [%]
Mesophilic sludge (37°C)	2.1±0.6	2.2±0.9	2.8±0.9
Thermophilic sludge (55°C)	8.3±1.4	8.4±1.6	8.5±1.9

Table 3

Crystallization temperature (T_c), crystallinity (X_c) and melting point (T_m) of PBAT films before and after biodegradation under mesophilic (37°C) and thermophilic anaerobic condition (55°C) at various cooling rates.

Sample	Cooling rate [°C/min]	T_c [°C]	X_c [%]	T_m [°C]
sample before biodegradation	10	72.69	8.11	122.25
	20	62.61	8.55	120.73
	30	56.42	9.21	119.93
	40	52.03	11.88	120.13
	50	46.61	8.08	-
sample after biodegradation at 37 °C	10	77.97	7.81	123.46
	20	68.16	8.25	123.42
	30	60.75	8.96	123.75
	40	55.31	11.15	124.19
	50	49.70	8.80	-
sample after biodegradation at 55 °C	10	111.62	9.72	129.82
	20	108.12	10.62	128.12
	30	105.65	11.69	126.67
	40	97.38	12.04	125.51
	50	94.80	11.38	-

Table 4

Avrami parameters of nonisothermal crystallization of PBAT films before and after biodegradation under mesophilic (37°C) and thermophilic anaerobic condition (55°C)

Sample	Cooling rate [°C/min]	n	Z [s ⁻ⁿ]	K [s ⁻¹]	t _{1/2} [s]
Sample before biodegradation	10	2.9894	1.66e-6	0.0117	75.51
	20	3.3451	1.58e-6	0.0184	44.97
	30	3.4537	3.56e-6	0.0264	35.36
	40	3.1507	1.94e-5	0.0320	28.01
	50	3.5096	8.72e-6	0.0362	24.64
sample after biodegradation at 37 °C	10	2.9062	2.36e-6	0.0116	77.48
	20	3.1656	3.10e-6	0.0182	51.51
	30	3.2507	5.81e-6	0.0245	37.14
	40	3.3916	5.73e-6	0.0285	29.36
	50	3.2279	2.47e-5	0.0374	25.42
sample after biodegradation at 55 °C	10	2.1897	1.26e-5	0.0058	142.79
	20	2.5807	1.44e-5	0.0133	62.88
	30	2.7998	2.83e-5	0.0237	44.56
	40	2.9981	2.54e-5	0.0293	31.42
	50	3.2094	1.80e-5	0.0332	27.63

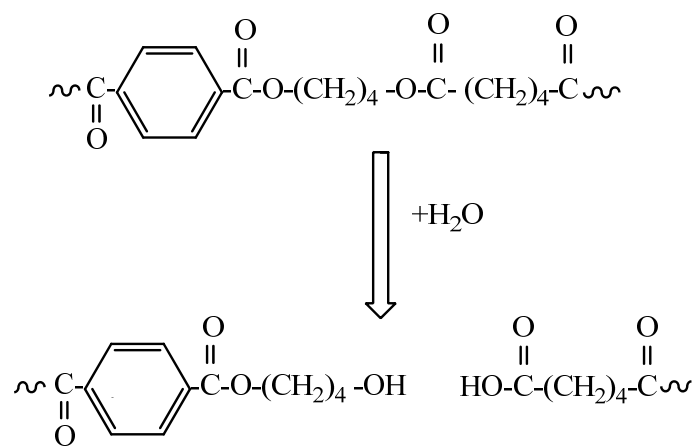


Fig. 1. Hydrolytic degradation of PBAT.

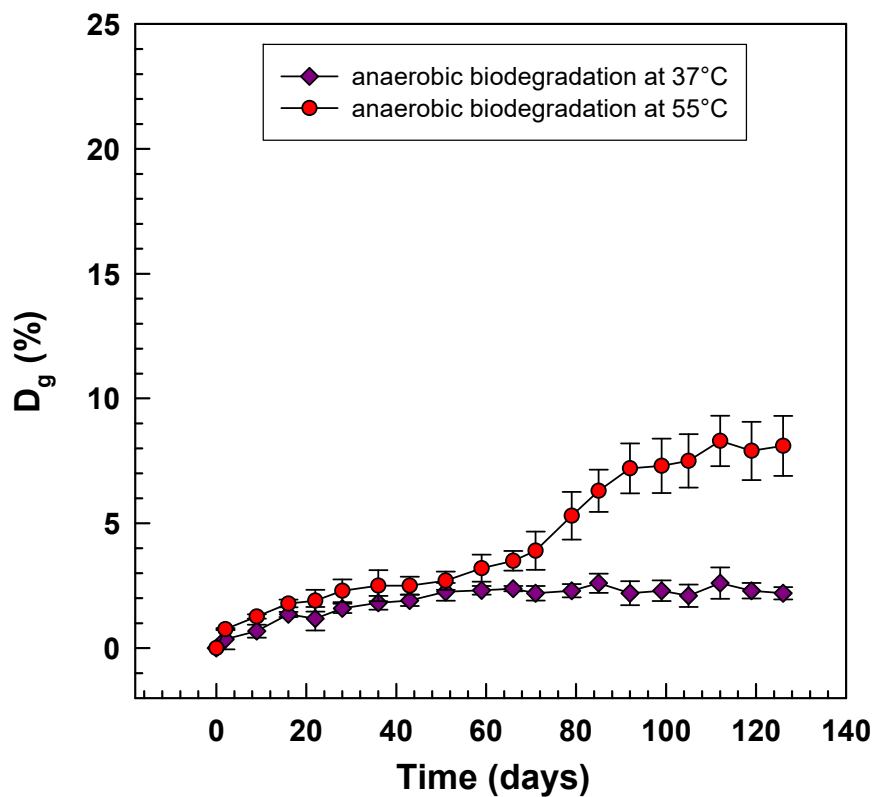


Fig. 2. Degree of biodegradation by biogas production (D_g) of PBAT under mesophilic anaerobic (37°C) and thermophilic anaerobic condition (55°C).

D_g (degree of biodegradation by biogas production) is expressed as the percentage of carbon in form of methane and carbon dioxide, generated out of theoretical amount of organic carbon in the polymer. Error bars correspond to twice standard deviation ($n = 3$).

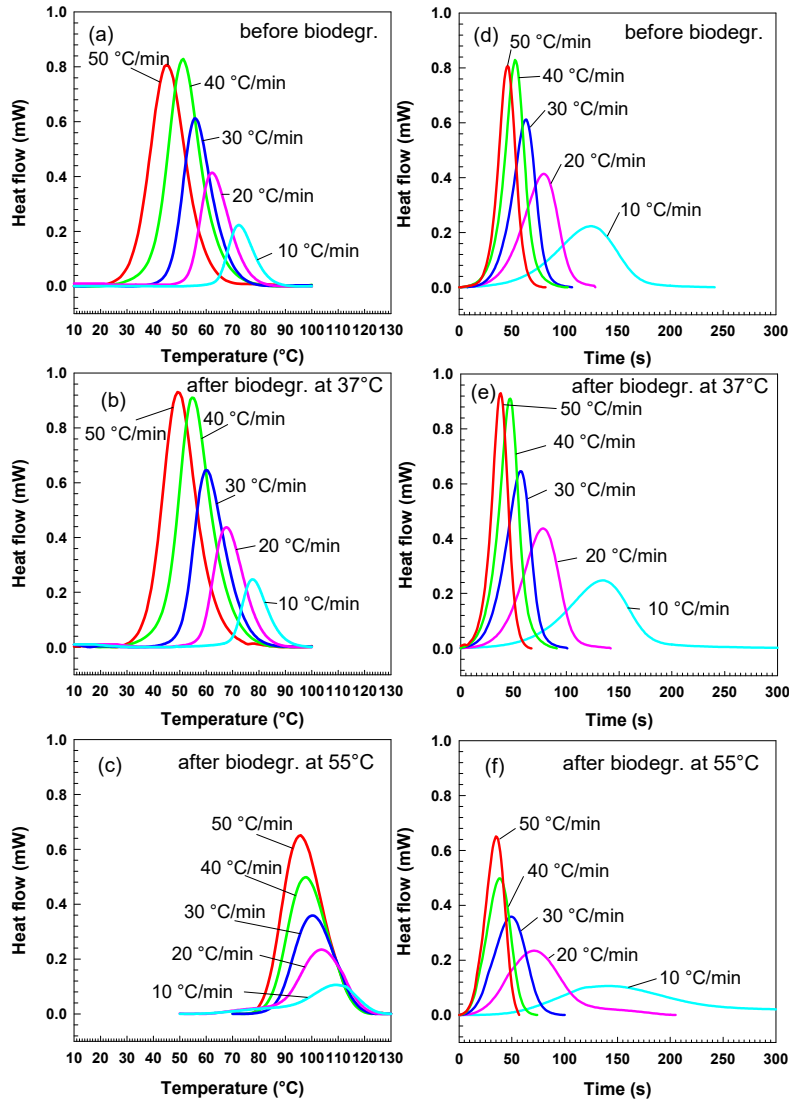


Fig. 3 Nonisothermal crystallization of PBAT at various cooling rates by DSC. (a,d) original sample, (b,e) after biodegradation in mesophilic anaerobic sludge at 37°C (c,f) after biodegradation in thermophilic anaerobic sludge at 55°C.

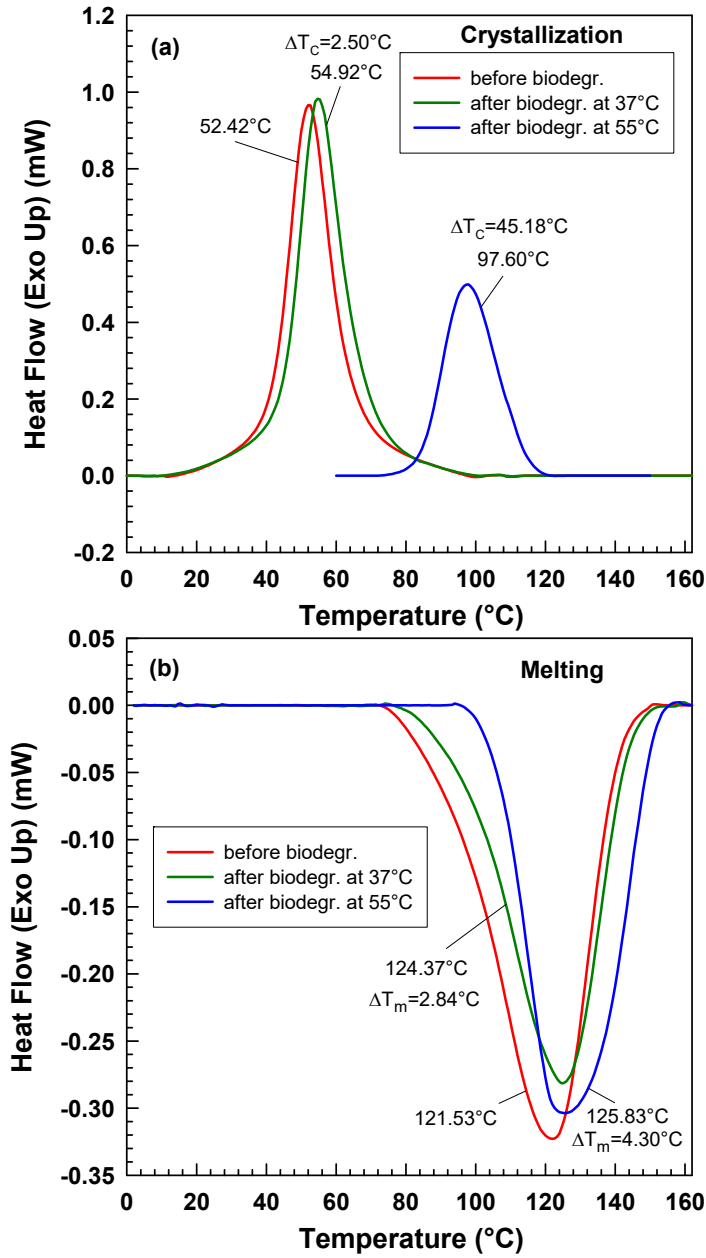


Fig. 4. Shift of (a) crystallization temperature T_c and (b) melting point T_m for PBAT during second heating and cooling at 40 °C/min.

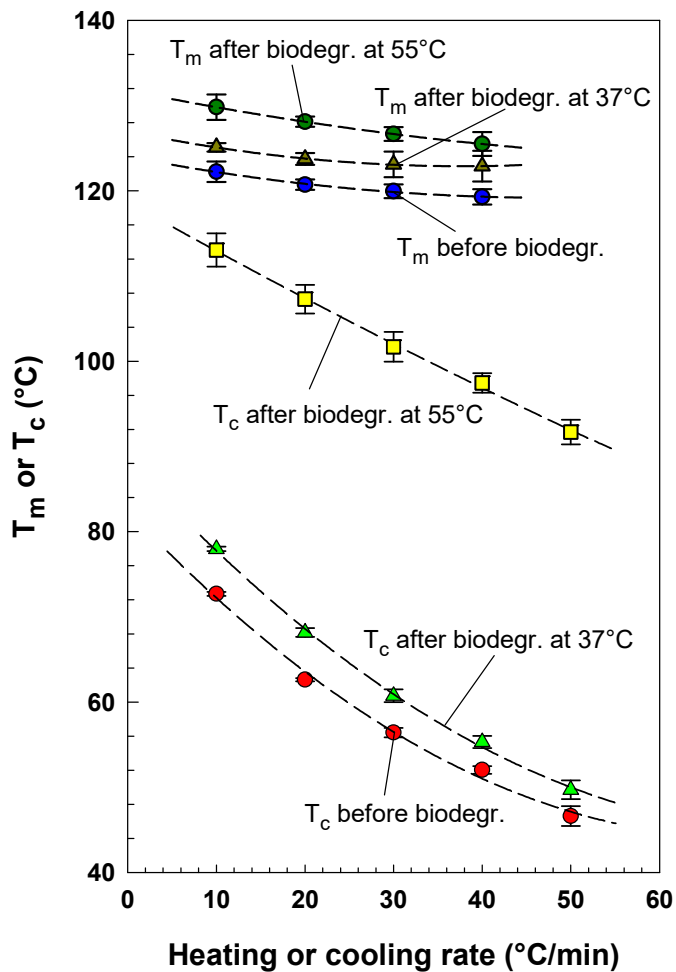


Fig. 5. Change of crystallization temperature T_c and melting temperature T_m caused by biodegradation of PBAT as a function of heating (cooling) rate.

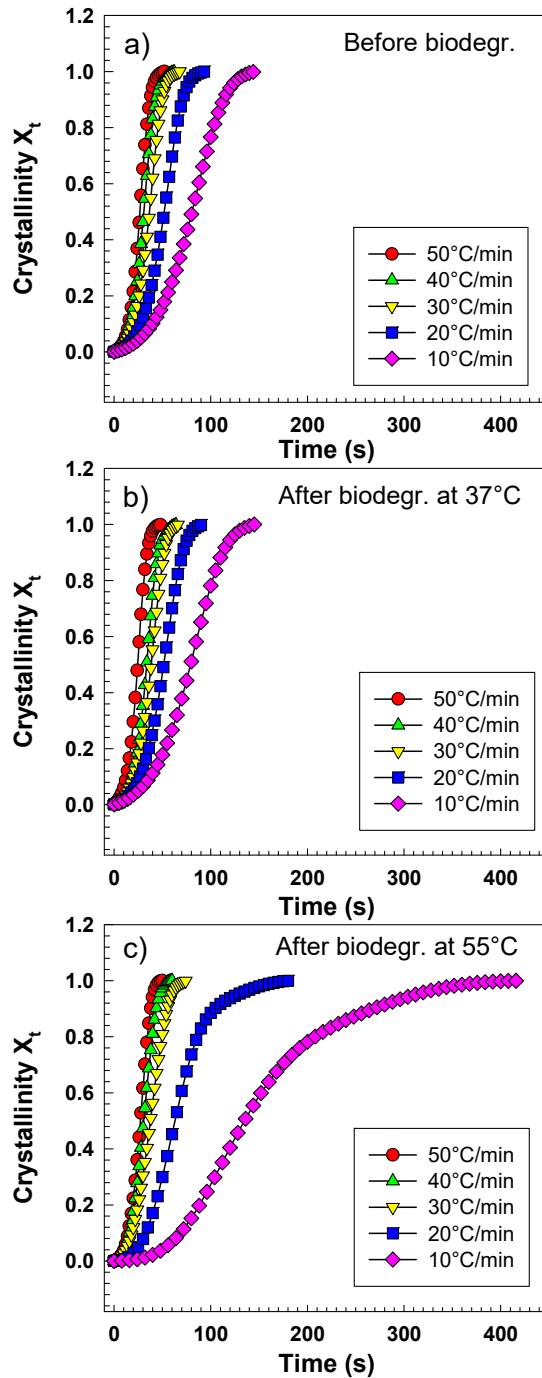


Fig. 6. Relative crystallinity (X_t) as a function of time during nonisothermal crystallization for PBAT (a) before biodegradation (b) after biodegradation in mesophilic anaerobic sludge at 37°C, (c) after biodegradation in thermophilic anaerobic sludge at 55°C.

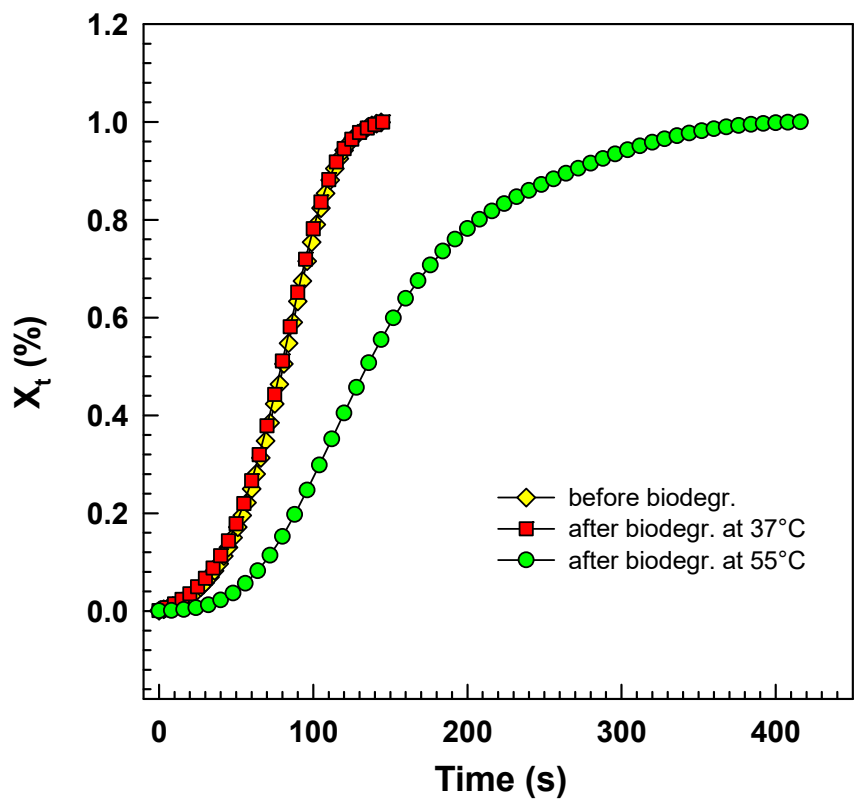


Fig. 7. Comparison of relative crystallinity (X_t) development for PBAT before and after biodegradation at cooling rate 10 °C/min.

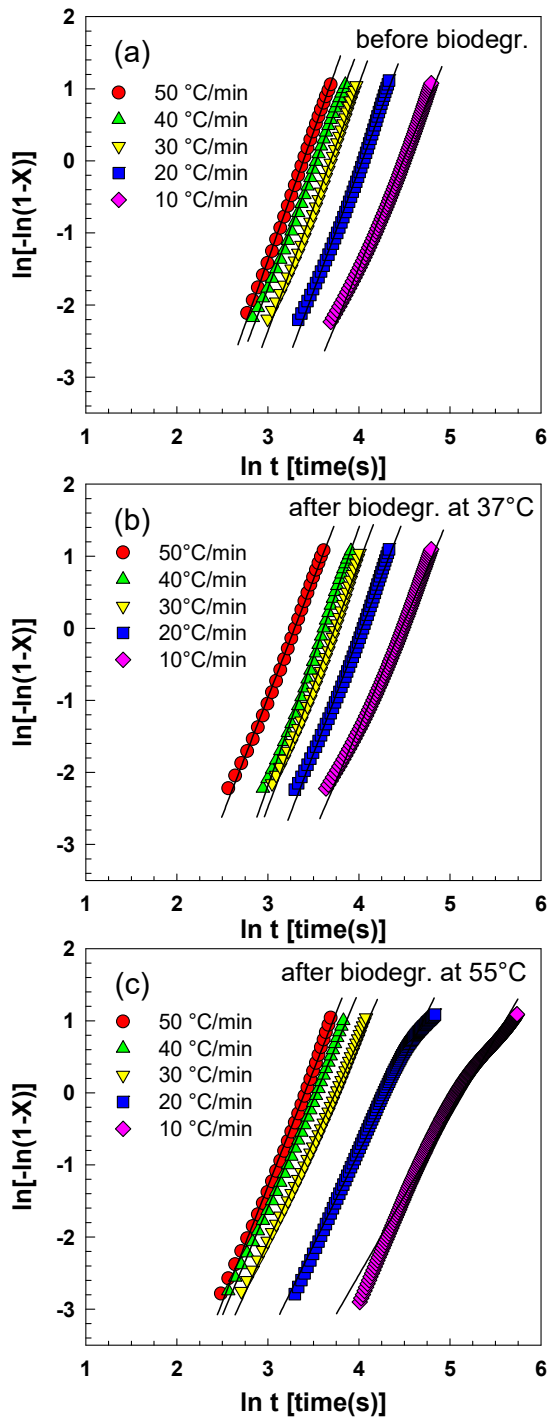


Fig. 8. Plots according to Avrami's equation for PBAT (a) before biodegradation (b) after biodegradation at 37 °C (c) after biodegradation at 55 °C

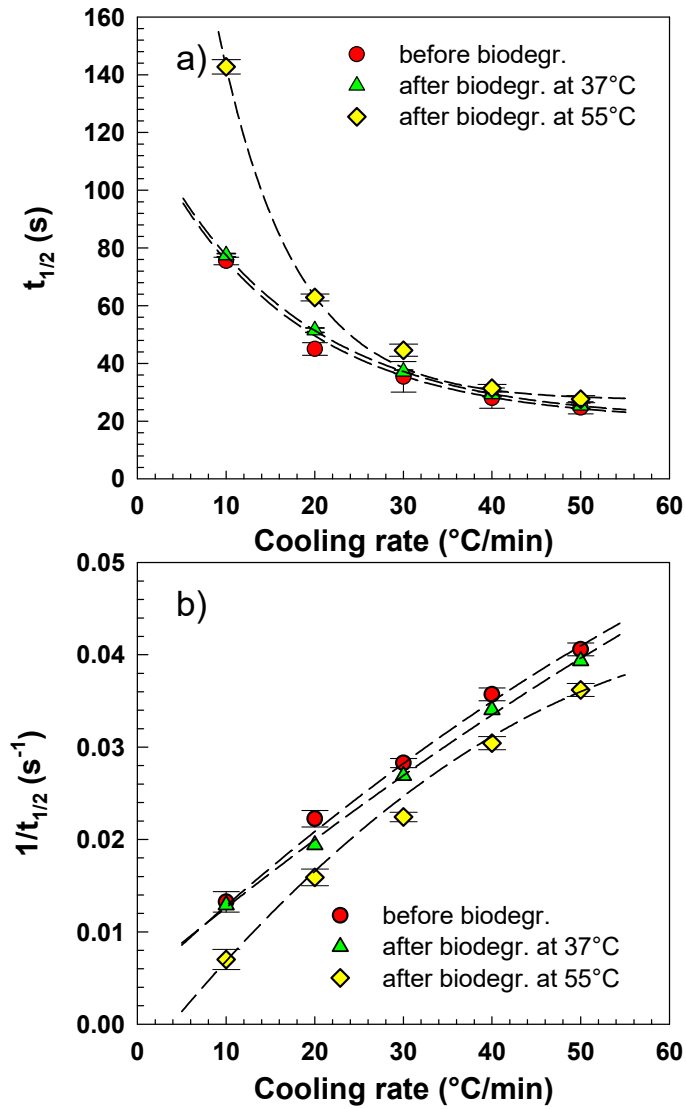


Fig. 9 (a) Half time of crystallization $t_{1/2}$ and (b) crystallization kinetics $1/t_{1/2}$ as a function of cooling rate before and after biodegradation under mesophilic (37°C) and thermophilic anaerobic conditions (55°C)

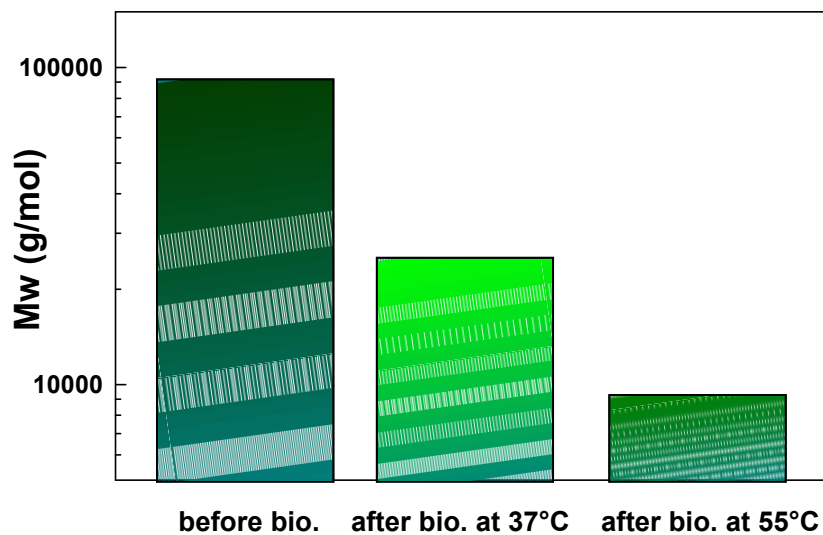
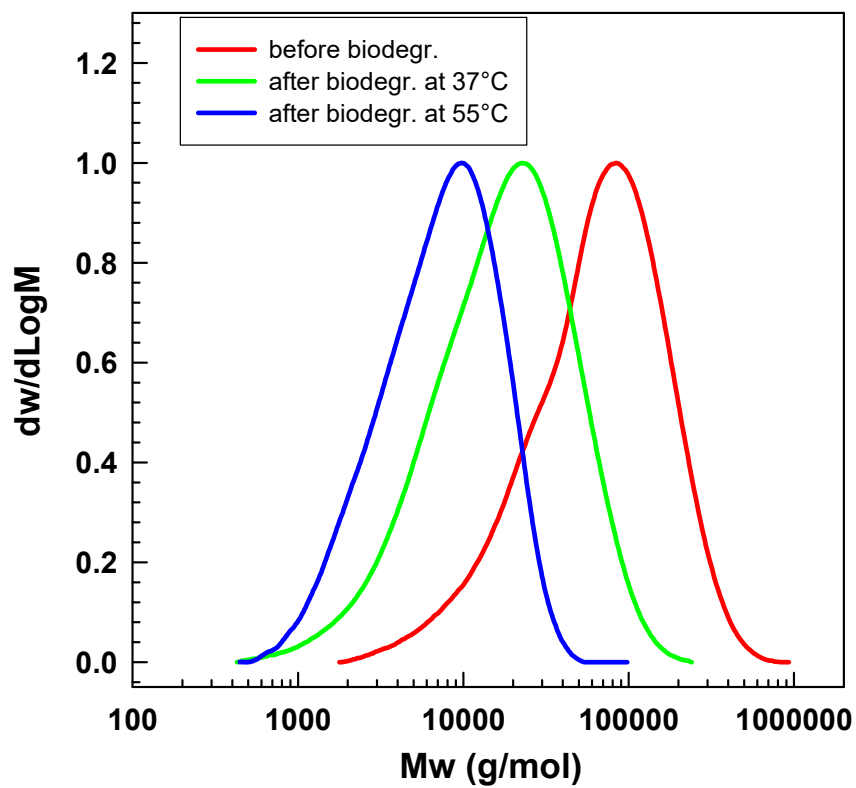


Fig. 10 Molecular weight distribution of PBAT before and after biodegradation under mesophilic (37°C) and thermophilic anaerobic conditions (55°C).

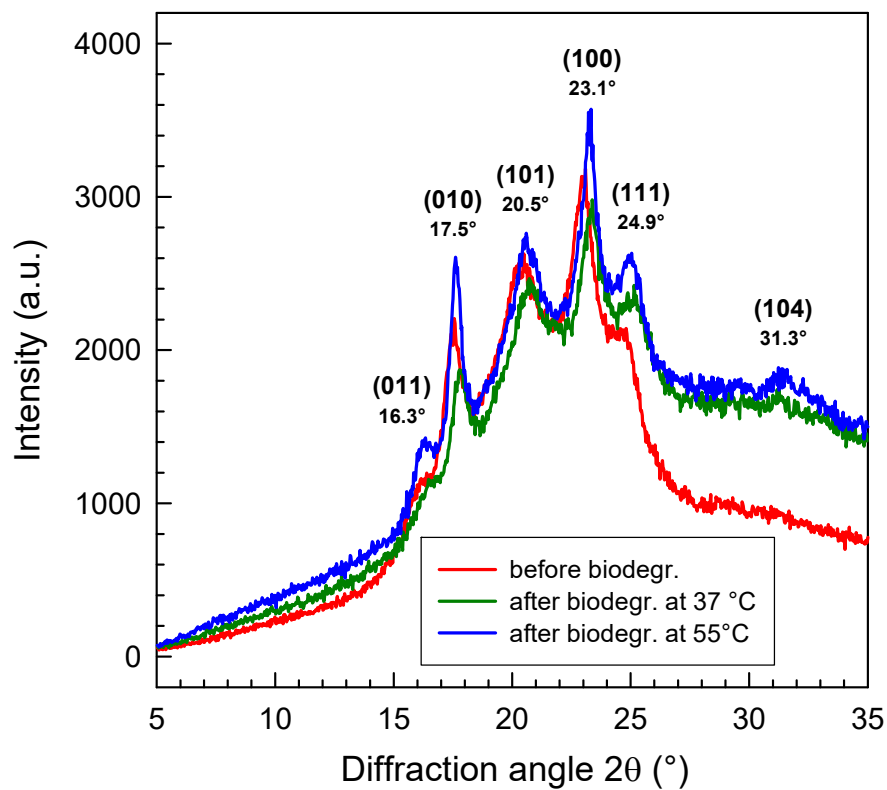


Figure 11. XRD diffraction patterns for PBAT before and after biodegradation under mesophilic (37°C) and thermophilic anaerobic conditions (55°C).